Towards sustainable and efficient data collection using dynamic sampling for gravel road condition assessment

Sustainable and Resilient Infrastructure

ISSN: 2378-9689 (Print) 2378-9697 (Online) Journal homepage: www.tandfonline.com/journals/tsri20

Towards sustainable and efficient data collection using dynamic sampling for gravel road condition assessment

Keegan Mbiyana , Hatem Algabroun , Maxime Riou , Mirka Kans , Rammohan Kodakadath Premachandran & Lars Håkansson

To cite this article: Keegan Mbiyana , Hatem Algabroun , Maxime Riou , Mirka Kans , Rammohan Kodakadath Premachandran & Lars Håkansson (05 Aug 2026): Towards sustainable and efficient data collection using dynamic sampling for gravel road condition assessment, Sustainable and Resilient Infrastructure, DOI: 10.1080/23789689.2026.2713294

To link to this article: https://doi.org/10.1080/23789689.2026.2713294

Published online: 05 Aug 2026.

SUSTAINABLE AND RESILIENT INFRASTRUCTURE
https://doi.org/10.1080/23789689.2026.2713294

Towards sustainable and efficient data collection using dynamic sampling for gravel road condition assessment

Keegan Mbiyana [a], Hatem Algabroun [a], Maxime Riou [b], Mirka Kans [a,c], Rammohan Kodakadath Premachandran [a] and Lars Håkansson [a]

[a]Department of Mechanical Engineering, Linnaeus University, Växjö, Sweden; [b]EPITA: School of Computer Engineering, Paris, France; [c]Department of Technology Management and Economics, Chalmers University of Technology, Gothenburg, Sweden

ABSTRACT
This paper examines a dynamic sampling technique for optimising the collection and storage of gravel road condition data by reducing redundancy while preserving accuracy. Advances in sensor technology and Information and Communication Technology (ICT) enable large-scale condition assessment but generate vast amounts of data, making efficient collection and storage essential. The Dynamic Sampling Rate Algorithm–Parametric Machine Learning Optimisation (DSRA-PMLO) was applied to simulated datasets and vehicle vibration response (VVR) signals collected using an Integrated Electronics Piezo-Electric (IEPE) accelerometer on three gravel roads with varying surface conditions. The algorithm was evaluated using error thresholds of 5–50%. Results show that DSRA-PMLO substantially reduces data volume without significant information loss. At a 20% error threshold, approximately 50% of the original data was sufficient for accurate condition assessment, while faults including potholes, corrugation, and loose gravel remained reliably detectable. Reduced data collection also lowers storage, bandwidth, and energy requirements.

ARTICLE HISTORY
Received 25 April 2025
Accepted 28 July 2026

KEYWORDS
Condition assessment; data reduction; dynamic sampling; fault detection; gravel road; vehicle vibration response

1. Introduction

Gravel roads constitute a significant portion of the global road network and are crucial infrastructure for rural development and well-being. In Sweden, private and state-owned gravel roads account for approximately 20% of the total national road network, which spans around 580,000 kilometres, excluding forest roads (Kans, Campos, & Håkansson, 2020). Compared to paved roads, gravel roads deteriorate more rapidly and are more prone to dust and road surface irregularities, such as potholes, corrugations, rutting and loose gravel. These irregularities contribute to accelerated vehicle wear and tear, reduced ride comfort, increased travel time, and increased fuel consumption for fuel-powered engines (Mbiyana et al., 2022). Moreover, gravel road surface irregularities pose a significant risk of traffic accidents, imposing substantial societal costs (Bardal & Jørgensen, 2017; Hurtig et al., 2023). Potholes, corrugations, and rutting can significantly reduce vehicle stability and control, ultimately compromising safety. Additionally, dust can impair the driver's vision (Albatayneh, Forslöf, & Ksaibati, 2019; Rafiei et al., 2025). In Sweden, accidents related to gravel roads are estimated to cost around EUR 13.4 billion annually, or 2.6% of the GDP (International Transport Forum, 2021; Swedish Civil Contingencies Agency [MSB], 2012). Furthermore, the environmental and health damage of dust from gravel roads is estimated to cost USD 1,500/km/year (Albatayneh, Forslöf, & Ksaibati, 2019; Aleadelat & Ksaibati, 2018).

Regular maintenance of gravel roads is essential to keep the road network in good condition. While national strategies and management practices differ, current maintenance strategies primarily rely on predetermined maintenance activities (Edvardsson, Lundberg, & Sjögren, 2015). However, maintenance needs vary depending on traffic and weather conditions (Alzubaidi & Magnusson, 2002), highlighting the need for more adaptive and data-driven strategies to optimise road performance (Mbiyana, Kans, & Campos, 2021). Human visual inspection and manual assessment have traditionally been the primary

CONTACT Keegan Mbiyana keegan.mbiyana@lnu.se

methods for monitoring road conditions, including gravel roads (Hong Pham et al., 2024). However, these approaches are prone to human error, inconsistent, and resource-intensive (Mbiyana et al., 2022). Advancements in digital technologies, including Information and Communication Technology (ICT) and the Internet of Things (IoT), now enable large-scale data collection on infrastructure conditions (Ben-Aboud et al., 2021; Hong Pham et al., 2024). This data can be processed, analysed, visualised, and fed into intelligent algorithms to assess and predict road conditions (Hong Pham et al., 2024; Mbiyana, Kans, & Campos, 2021).

Participatory condition data collection could be a cost-effective approach for evaluating the condition of gravel roads by enabling broader coverage and large-scale data acquisition (H. Kim, Ahn, & Yang, 2016; Nunes & Mota, 2019). It has already been successfully applied in fields such as personal health tracking, air quality monitoring, real-time traffic analysis, and noise mapping (Nunes & Mota, 2019). While not a new concept, its application in road maintenance remains limited. In (Mbiyana & Kans, 2024), a participatory data collection approach is proposed to support maintenance planning and decision-making, potentially improving unpaved road management. Advances in sensors and digitalisation are expected to further enhance data-driven approaches for gravel road assessment (Nižetić et al., 2020). The transport sector generally contributes significantly towards greenhouse gas emissions (Pampolina et al., 2024). Thus, leveraging management strategies that integrate sensors and digitalisation could improve real-time condition monitoring and forecasting and minimise the environmental impact, leading to more efficient maintenance strategies.

Nevertheless, large amounts of data might pose new challenges for data collection and storage systems. As large amounts of gravel road condition data are collected over time, the demand for storing and managing the data vis-à-vis data centres increases. Therefore, more energy would be required for cooling systems, increasing energy consumption and carbon emissions, with research showing that big data centres consume up to 1,000 kWh per square meter (Ahmed, Bollen, & Alvarez, 2021). Moreover, the processing capabilities and transmission networks to the storage centre are strained, and thus, more energy-efficient and sustainable transmitting and computing solutions would be needed (Algabroun, 2020). Furthermore, gravel roads are often found in remote areas where internet connections can be challenging. Therefore, the real-time transmission of large amounts of condition data collected to the data centre is affected, thus demanding a large offline storage capacity. Dynamic or adaptive sampling, sometimes referred to as data compression algorithm techniques (Daniel et al., 2021), can be a solution for efficient data collection and storage.

Therefore, a dynamic sampling algorithm can be integrated into a participatory data collection system to remove the accumulated redundant data before transmitting the data for storage. This paper examines the impact of a dynamic sampling technique in reducing redundant data before storage and subsequent analysis. Given the absence of an adaptive sampling technique specifically tailored for vibration measurements, this research applies and adapts the Dynamic Sampling Rate Algorithm – Parametric Machine Learning Optimisation (DSRA-PMLO), previously proposed by Algabroun and Håkansson, (2025), to vehicle vibration response data for gravel road condition assessment. The study evaluates the applicability and performance of DSRA-PMLO in the context of gravel roads.

Adaptive sampling techniques dynamically adjust the sampling interval according to changes in the acquired signal or data stream, thereby reducing redundant or unnecessary data while maintaining the application's required coverage and information precision (Algabroun, 2020; Ben-Aboud et al., 2021; Rault, Abdelmadjid, & Challal, 2014). Consequently, adaptive sampling can be integrated into participatory condition monitoring systems to minimise the volume of data transmitted and stored, improving data collection efficiency. This is particularly important for large-scale participatory monitoring of gravel roads, which generates substantial volumes of vehicle vibration response (VVR) data, leading to increased storage, transmission, and energy requirements. Although adaptive sampling algorithms have been developed for general IoT and environmental monitoring applications (Algabroun, 2020; Algabroun & Håkansson, 2025), their applicability to vibration-based gravel road condition assessment has not yet been investigated. Furthermore, the highly non-stationary nature of VVR signals requires verification that adaptive sampling preserves the diagnostic information necessary for reliable fault detection and condition assessment.

Therefore, this study applies the previously developed Dynamic Sampling Rate Algorithm – Parametric Machine Learning Optimisation (DSRA-PMLO) (Algabroun & Håkansson, 2025) to VVR signals as a proof of concept for vibration-based gravel road condition assessment. Rather than proposing a new adaptive sampling algorithm, the study evaluates the suitability of DSRA-PMLO for this application by validating whether dynamically sampled and reconstructed VVR signals preserve the information required for reliable condition assessment. This is achieved through an application-oriented validation based on complementary performance measures, including approximation error (MAAPE), mean-square acceleration, frequency sub-band analysis, power spectral density estimates, and the detectability of gravel road defects. In addition, the study establishes practical approximation-error thresholds that balance data reduction with condition assessment accuracy.

The main contributions of this study are threefold. First, it extends the application of the previously developed DSRA-PMLO algorithm to vehicle vibration response signals for gravel road condition assessment. Second, it evaluates and validates the suitability of DSRA-PMLO as an adaptive sampling technique in vibration-based condition monitoring using complementary measures of signal reconstruction accuracy, spectral preservation, and fault detectability. Third, based on experimental validation using measured VVR data collected from gravel roads with different surface conditions, it establishes practical approximation-error thresholds that achieve substantial data reduction while maintaining reliable gravel road condition assessment.

To achieve this, the research addresses three research questions:

(1) How can DSRA-PMLO improve gravel road condition assessment using vehicle vibration response (VVR) signals?
(2) What is the effect of DSRA-PMLO on fault detection (e.g., potholes, corrugations, and loose gravel) in gravel road condition assessment?
(3) What level of approximation accuracy is required for DSRA-PMLO to ensure sufficient coverage and information precision for identifying gravel road faults?

The remainder of the paper is organised as follows: the next section (Section II) discusses the signal processing and analysis of the VVR data, followed by Section III, where the adaptive sampling and the fundamental operation of DSRA-PMLO are presented. The research methodology is presented in Section IV, and the study results, i.e., the implementation and evaluation of DSRA-PMLO on randomly generated signals and real-case VVR data, are presented in Section V. The algorithm's performance on the vehicle VVR data is evaluated and discussed in Section VI. Lastly, in Section VII, conclusions are drawn, along with suggestions for future work.

2. Signal processing and analysis of vehicle vibration response data

Vehicle vibration response (VVR) data collected from vehicle-mounted sensors have been widely used to assess paved road conditions (Wang, Zhou, & Yang, 2022) and have recently emerged as a promising approach for evaluating gravel road conditions (Mbiyana & Kans, 2024). As a vehicle drives on a gravel road with irregularities, potholes, and heterogeneous gravel road surfaces, distinct vibration responses are triggered, differing in intensity from those on smooth surfaces. The vibrations perceived by road users can serve as indicators of the road condition, specifically roughness. Loprencipe and Zoccali (Loprencipe & Zoccali, 2017) demonstrated that the wavelength profile of a road directly influences the perceived comfort level by the road user. Building on this, various signal processing and analysis techniques have been developed to assess road conditions by linking surface irregularities to user discomfort. These include machine learning approaches (Gorges, Öztürk, & Liebich, 2019; Shtayat, Moridpour, Best, & Abuhassan, 2023), vehicle model-based and profile reconstruction (Rana & Asaduzzaman, 2021), and statistical methods (W. Liu et al., 2020; Yu, Fang, & Wix, 2022).

Analysing variations in the statistical properties of vehicle vibrations using time series analysis can provide insights into gravel road irregularities (Žuraulis et al., 2021). When driving on a gravel road, the vehicle's vibration response can typically be characterised as a random signal. For a second-order ergodic random signal x(t), the mean square value, $r_x(0) = E[x^2(t)]$ of x(t), where t represents time, can be estimated based on the sampled version of the random signal x(n), n is discrete, according to the time average (Vaidyanathan, 1993) as:

$$\hat{r}_x(0) = \frac{1}{N_a}\sum_{n=0}^{N_a-1} x^2(n) \tag{1}$$

N_a being the number of samples in the average time, $t = nT_s$, and T_s is the sampling time interval. The variance s_x^2 for the signal x(n) may be estimated (Papoulis & Pillai, 2002) as:

$$\hat{s}_x^2 = \frac{1}{N_a}\sum_{n=0}^{N_a-1} (x(n) - \hat{m})^2 \tag{2}$$

$\hat{m}$ being an estimate of the mean value of the random process. However, for a non-stationary random signal x(n) with time-varying mean square values, a moving average of the squared signal samples may provide an estimate of the time-varying properties of the mean square values of the signal according to (Bendat & Piersol, 2012; Shtayat, Moridpour, Best, & Daoud, 2023) as:

$$\hat{E}\left[x^2(n)\right] = \frac{1}{N_a}\sum_{l=n-\frac{N_a}{2}}^{n+\frac{N_a}{2}-1} x^2(l), n\hat{I}\left\{\frac{N_a}{2}, \frac{N_a}{2}+1, \ldots\right\} \tag{3}$$

The average is produced over N_a samples and with the average time $T_a = N_a T_s$. The moving average low-pass filtering of the squared signal $x^2(n)$ will attenuate the squared signal at higher frequencies, inversely proportional to the averaging time, while passing the squared signal within the filter's passband unattenuated (Shtayat, Moridpour, Best, & Daoud, 2023). The averaging time T_a is selected as a compromise between a time interval bias error and random error, for instance, by a trial and error-based method (Andrén et al., 2004). By dividing the signal into adjacent frequency bands with the aid of band-pass filters defined based on the Discrete Fourier Transform (DFT), having the impulse response functions h_k^{DFT}, more information concerning the non-stationary second-order statistical properties of the random squared signal $x^2(n)$ (Vaidyanathan, 1993), in this case, the vertical vibration response can be obtained as:

$$h_k^{DFT} w(n) = \begin{cases} w(N-1-n)e^{-\frac{j2\pi k(N-1-n)}{N}}, n = 0, 1, \ldots, N-1 \\ 0, otherwise \end{cases} \tag{4}$$

w(n) is the window function, e.g., a Hanning window, $k = 0, 1, \ldots, \frac{N}{2} - 1$ is the discrete centre frequency of the band-pass filters and $f = k * \frac{F_s}{N}$ is the actual frequency at the normalised discrete frequency k. N is the impulse response length and the $\frac{N}{2}$ band-pass filter has the same bandwidth. Filtering the signal $x(n)$ with the band-pass filters $h_k^{DFT} w(n), k = 0, 1, \ldots, \frac{N}{2} - 1$ produces $\frac{N}{2}$ complex-valued signals $y_k(n)$. The instantaneous power in each frequency sub-band with discrete centre frequency, $k = 0, 1, \ldots, \frac{N}{2} - 1$, at time n, is produced by scaling the squared magnitude of these complex-valued signals (Vaidyanathan, 1993), according to (5):

$$p_k(n) = \begin{cases} \frac{1}{N\sum_{l=0}^{N-1} w^2(l)} |y_k(n)|^2, k = 0 \\ \frac{2}{N\sum_{l=0}^{N-1} w^2(l)} |y_k(n)|^2, 0 < k \leq \frac{N}{2} - 1 \end{cases} \tag{5}$$

3. Adaptive sampling

The challenges of large-scale condition data collection, such as data overload and heightened energy consumption, can be mitigated by reducing the amount of data collected using various methods, including adaptive sampling algorithms (Alippi et al., 2010; Rodriguez-Pabon et al., 2022), by dynamically adjusting data selection criteria to enhance energy efficiency. Many adaptive sampling techniques exist, such as the utility-based sensing and communication protocol (Padhy et al., 2006), compressive data gathering (Luo et al., 2009) and model-based filtering approximate techniques (Chu et al., 2006). A balance between resource optimisation and adaptive solutions becomes imperative in tackling the complex landscape of data overload, energy consumption and sustainability. Several researchers have considered and explored adaptive sampling techniques for application in various fields, including wireless sensors (Algabroun, 2020), sensor networks (Lu et al., 2017) and energy-harvesting wireless devices (Gindullina, Badia, & Vilajosana, 2020).

Each adaptive sampling technique possesses distinctive strengths, weaknesses, and methodologies for approximation accuracy and data reduction. High approximation accuracy usually demands higher sampling rates (Lu et al., 2017). However, depending on the application, higher approximation accuracy is not always required; therefore, allowing a predetermination of approximation accuracy can enhance efficiency (Algabroun & Håkansson, 2025). DSRA-PMLO was selected in this study because it allows for predetermining the approximation accuracy of the monitored signal. In addition, it has low computational demands and scales efficiently, even for long-term data collection tasks (Algabroun & Håkansson, 2025). For more comprehensive surveys of adaptive sampling techniques, see (Alippi et al., 2010; Giouroukis et al., 2020).

3.1. Brief overview of the Dynamic Sampling Rate Algorithm - Parametric Machine Learning Optimisation (DSRA-PMLO)

A suitable sensor with an analogue electrical output signal is generally used when measuring a physical quantity, such as the vehicle vibration response. The sensor's analogue output signal is connected to a data acquisition system, and the sensor output signal is converted to a digital signal by an analogue-to-digital converter, which generally uses a fixed sampling frequency (Bendat & Piersol, 2012). As the collected signals are a series of discrete data points representing the continuous signal, an adaptive algorithm such as the DSRA-PMLO minimises the samples by, in principle, dynamically allocating the data points at the optimum locations. The information in the dynamically sampled signal should represent the original signal as accurately as possible (Algabroun, 2020).

While the monitored signal can change dynamically, the sampling rate remains static. DSRA-PMLO adjusts the sampling rate based on the events detected in the signal. Whenever there is a variation in the monitored signal, the sampling rate adjusts accordingly. When the signal is static, the sampling rate is reduced to an optimal rate. The algorithm is built with two turning parameters: E, the exploratory parameter, which explores changes in the signal and S, the severity parameter, which determines the severity of the changes based on the slope defined by the two consecutive data points. The Time Between Measurements (TBM) can then be formulated as follows:

$$TBM = E - \left(\left| S * \frac{(y(t_i) - y(t_{i-1}))}{(t_i - t_{i-1})} \right| \right) \tag{6}$$

However, to avoid negative values for TBM, (6) is transformed with the aid of ε, a small positive value (~0), so that $TBM > 0$ always.

$$TBM = max\left\{ \varepsilon, E - \left(\left| S * \frac{(y(t_i) - y(t_{i-1}))}{(t_i - t_{i-1})} \right| \right) \right\} \tag{7}$$

The next measurement time, t_{i+1} can then be defined based on TBM as follows:

$$t_{i+1} = t_i + TBM \tag{8}$$

Combining (7) and (8) yields:

$$t_{i+1} = t_i + max\left\{ \varepsilon, E - \left(\left| S * \frac{(y(t_i) - y(t_{i-1}))}{(t_i - t_{i-1})} \right| \right) \right\} \tag{9}$$

For further information on derivations of Equations 6–9, see (Algabroun, 2020; Algabroun & Håkansson, 2025).

The objective is to adjust the tuning parameters E and S in the DSRA parametric model to achieve the minimum number of samples that allows for the approximation of a signal with the required accuracy without violating the constraint value of pattern similarity. Generally, the higher the demanded accuracy, the higher the sampling cost. Moreover, different applications have different accuracy demands on the approximated signals. Accuracy demand as an input variable provides the algorithm with specific domain customisation for further efficiency in data collection. DSRA-PMLO uses the recorded data to achieve dynamic sampling that does not violate the predetermined approximation constraint.

The measurement points are selected optimally from the sensor measurements $y(t_1)\ldots,y(t_N)$ representing a continuous-time signal $s(t), t \in [0,T]$, by choosing the minimum number of measurement times $t_1\ldots,t_{Nmin}$, and obtain sensor values $y(t_1),\ldots,y(t_{Nmin})$, such that the interpolated function $I(y(t_1),\ldots,y(t_{Nmin}))$ closely approximates the underlying signal $s(t)$. The closeness of the approximation, e, is measured using a quality metric e_{MAAPE}, the mean arctangent percentage error (MAAPE). MAAPE addresses several limitations of traditional error metrics, such as normalised mean error (NME), root mean square error (RMSE), mean relative error (MRE), mean absolute error (MAE), and the widely used mean absolute percentage error (MAPE) (Algabroun & Håkansson, 2025). These limitations include instability with zero or near-zero actual values and asymmetric error penalisation (Algabroun & Håkansson, 2025). MAAPE is particularly suitable for assessing approximation performance in dynamic sampling of vehicle vibration response data, and one of its key advantages is its intuitive interpretation as an absolute percentage error, as noted by Kim and Kim (S. Kim & Kim, 2016). For simplicity, throughout this paper, MAAPE will be treated and referred to as a percentage error (Algabroun & Håkansson, 2025).

$$e_{MAAPE} = \frac{1}{N}\sum_{i=1}^{N} arctan\left(\left|\frac{y(t_i)-\hat{y}(t_i)}{y(t_i)}\right|\right) for\ i = 1,\ldots,N \tag{10}$$

The optimisation problem involves a parameterised model, DSRA, for determining the measurement points, and the subsequent measurement time is determined based on given parameters E and S. The aim is to minimise the error, e_{MAAPE} between the interpolated function and the underlying signal, considering a maximum approximation error M. The number of measurements for the given E and S is denoted by (E,S), while $t_1(E,S),\ldots,t_{N(E,S)}(E,S)$ are the measurement points for the given E,S. The error metrics e_{MAAPE} are used to quantify the approximation quality for each as:

$$e_{MAAPE} = e(s(t), I(y(t\_1(E,S),\ldots,y\big(t_{\{Nmin(E,S)\}}(E,S)\big) \tag{11}$$

The aim is to minimise the number of measurements $N(E,S)$ and the approximation quality, measured by the error, e_{MAAPE}, does not exceed a specified threshold M. Thus, the objective function (E,S) of the optimisation problem is the minimum number of measurements $N_{min}(E,S)$ that do not violate the predetermined error threshold M.

Formally, the objective function is expressed as:

Objective: minimize $N(E,S)s.t.$:

$$e_{MAAPE} = e\big(s(t), I\big(y\big(t_1(E,S),\ldots,t_{NMin(E,S)}(E,S)\big)\big)\big) \leq M \tag{12}$$

If the required accuracy is not achieved by using the current parameters set, the objective function is set to positive infinity and can be mathematically expressed as follows:

$$N_{min}(E,S) = \begin{cases} N(E,S) & if\ e\big(s(t), I\big(y\big(t_1(E,S),\ldots,t_{Nmin(E,S)}(E,S)\big)\big)\big) \leq M \\ +\infty & if\ e\big(s(t), I\big(y\big(t_1(E,S),\ldots,t_{\mathrm{Nmin}(E,S)}(E,S)\big)\big)\big) > M \end{cases} \tag{13}$$

From the objective functions in (12) and (13), the function can be assumed to be complex, non-differentiable, discontinuous, and far from convex. For this reason, DSRA-PMLO employs a stochastic algorithm, that is, the Dual Simulated Annealing (DSA), and for further details of the optimisation technique of DSA and its relevance to the DSRA-PMLO, see (Algabroun & Håkansson, 2025).

DSRA-PMLO is integrated with quadratic interpolation to reconstruct the signal from non-uniform sampling. Quadratic interpolation is an effective method for reconstructing signals in scenarios requiring a balance between computational efficiency and signal accuracy. Research has shown that polynomial interpolation techniques, including quadratic forms, can facilitate the reconstruction of vibration signals and maintain accurate spectral representation, even with non-uniform sampling (Ntakpe et al., 2017). Additionally, studies on vibration control using point interpolation techniques demonstrate that quadratic terms can capture essential signal dynamics without significant distortion (G. R. Liu, Dai, & Lim, 2004). In this study, the accuracy of the reconstructed signals is evaluated using MAAPE. Furthermore, Power Spectral Density (PSD) estimates and Mean Square Acceleration (MSA) were combined with frequency sub-band filtering of the VVR to examine the accuracy of the reconstructed signals and ensure that the key features of the original signal are preserved, along with the detectability of faults.

3.2. The power spectral density estimate and aliasing

To ensure reliable condition assessment, spectral analyses such as the PSD estimates can be employed to compare the original and resampled signals (Davis & Lanterman, 2015). PSD estimate comparisons help verify whether the resampled signals have retained the properties of the original signal (Welch, 1967). The presence of unexpected peaks or the absence of specific peaks in the resampled signal may indicate aliasing effects. A sufficiently high dynamic resampling rate of the DSRA-PMLO, adaptable to varying signal characteristics, would prevent undersampling in critical sections of the vibration response.

According to (Welch, 1967), the Welch power spectral density estimator $\hat{P}_{xx}^{PSD}(f_k)$ is given by as;

$$\hat{P}_{xx}^{PSD}(f_k) = \frac{1}{F_s L N U_{PSD}} \sum_{l=0}^{L-1} \left| \sum_{n=0}^{N-1} w(n) x_l(n) e^{-j2\pi nk/N} \right|^2 ; \ f_k = \frac{k}{N} F_s \tag{14}$$

Where, $k = 0, \ldots, \frac{N}{2} - 1$, $x_l(\mathrm{n})$ are the segments of a time sequence, w(n) is the window used, L is the number of periodograms, N is the length of the periodogram or block length, F_s is the sampling frequency and U_{PSD} is the window-dependent effective analysis bandwidth normalisation factor, defined as;

$$U_{PSD} = \frac{1}{N} \sum_{n=0}^{N-1} (w(n))^2 \tag{15}$$

Analysing the resampled and reconstructed VVR signals for assessing the gravel road condition requires careful attention to aliasing. The dynamic sampling rate must be sufficient to prevent signal distortion and ensure accurate interpretation. Aliasing occurs when a signal is undersampled, causing higher-frequency components to be misinterpreted as lower frequencies (Davis & Lanterman, 2015). Therefore, the sampling rate must be at least twice the highest frequency present in a signal (Nyquist rate) to prevent aliasing distortion (Algabroun & Håkansson, 2025). Vehicle vibration signals offer insights into surface irregularities, such as loose gravel, corrugations, and potholes. Aliasing distortion in the resampled and reconstructed signals can misrepresent these faults, leading to an underestimation of the fault severity and misclassification of the road condition.

4. Methodology

This section begins with a brief description of the field experiment setup and data acquisition. It then outlines the step-by-step process of testing DSRA-PMLO on the simulated data, which was validated using the MAAPE. Lastly, the analysis procedure of the VVR signals before and after applying DSRA-PMLO is presented. Figure 1 provides a summary of the methodology.

4.1. Field experiment setup and data acquisition

Field experiments were conducted in the 2022 spring season in Växjö municipality, southern Sweden, on three gravel roads classified as Class 1 (very good condition), Class 2 (good condition), and Class 3 (poor condition) for Road 1, Road 2, and Road 3, respectively. The classification was based on the Swedish standard for gravel road classification, TDOK 2014:0135 (Swedish Transport Agency, 2014). The average distances covered on the test roads were 5.25 km, 3.60 km and 2.40 km for Roads 1, 2 and 3, respectively.

Road 1 had a few small potholes and some portions with loose gravel. Road 2 was compact but had a portion with corrugations and small potholes, while Road 3 had numerous potholes of varying sizes and loose gravel scattered throughout its entire length. A Brüel & Kjær Integrated Electronics Piezo-Electric (IEPE) Accelerometer Type 4507B, connected to the Supervisory Control and Data Acquisition (SCADA) data acquisition system, was used to collect the VVR data. The experimental setup in Figure 2 shows the IEPE Accelerometer (Figure 2(B)) connected to the SCADA system (Figure 2(A)), which is mounted on

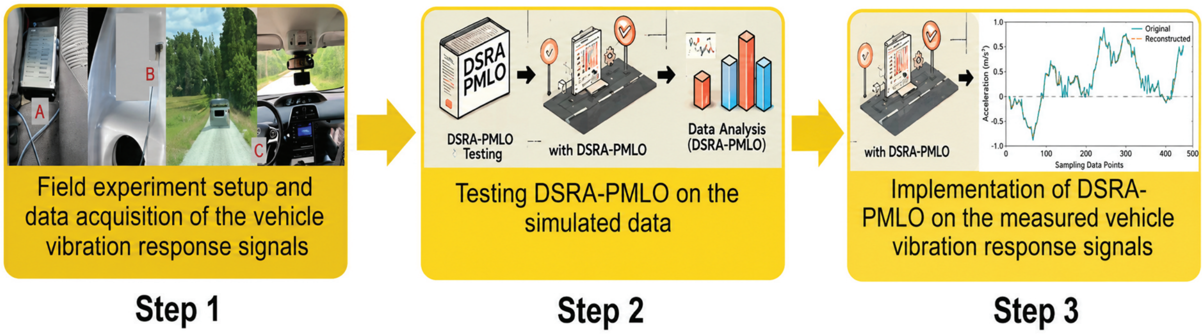

Figure 1. A summary of the methodology.

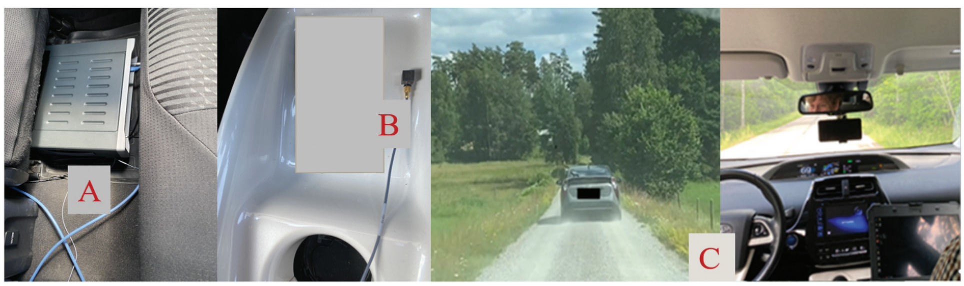

Figure 2. Field experimental setup.

a 2016 Toyota Prius hybrid model (Figure 2(C)). The mounting position of the IEPE Accelerometer enabled easy monitoring and the detection of the relative vibration response of the vehicle on both wheel paths, as well as reducing the impact of the engines' vibrations. IEPE accelerometers have wide applications in various industries for vibration measurement and are easy to install (Levinzon, 2015).

The VVR was acquired at a sampling frequency of 2048 Hz as the vehicle drove on the Test Roads at an average speed of 35 km/hr, and the collected VVR was stored in the Siemens Simcenter SCADA system for further processing.

4.2. Testing DSRA-PMLO on the simulated data

A comprehensive set of tests was conducted to evaluate the DSRA-PMLO's adaptability to varying signal complexity levels and validate its generalizability before it was applied to the VVR data. Distinct signals containing different frequency components with randomly generated frequencies and phases were generated. Consequently, each generated signal can be viewed as a realisation of a random process (Bendat & Piersol, 2012). Generally, the VVR signals collected when driving on gravel roads can be characterised as random. Based on experience from our previous works (Mbiyana & Kans, 2024; Mbiyana et al., 2024), gravel road irregularities such as potholes, corrugations and loose gravel can be detected within the bandwidth range of 0 to 1000 Hz.

This study utilises three representative test cases of signals randomly generated in Matlab, each containing 120, 300, and 600 frequency components distributed between 0 and 1200 Hz. The predetermined error thresholds, ranging from 0.5% to 5%, were used, representing the tolerances for approximation accuracy and directly affecting the algorithm's efficiency by determining how the sampling rate is adjusted. MAAPE was used to evaluate the algorithm's performance and assess the accuracy of the approximated signals. In addition, the reduction in samples was measured to quantify the efficiency of data collection.

The testing of DSRA-PMLO on the simulated data adopted the methodological framework from (Algabroun & Håkansson, 2025). The optimal values of E and S are obtained from the training data set and then applied to the testing dataset to obtain a compressed signal of the original signal. Figure 3 shows an example of the visualisation plot of the relationship between the number of measurements $N(E, S)$ and the

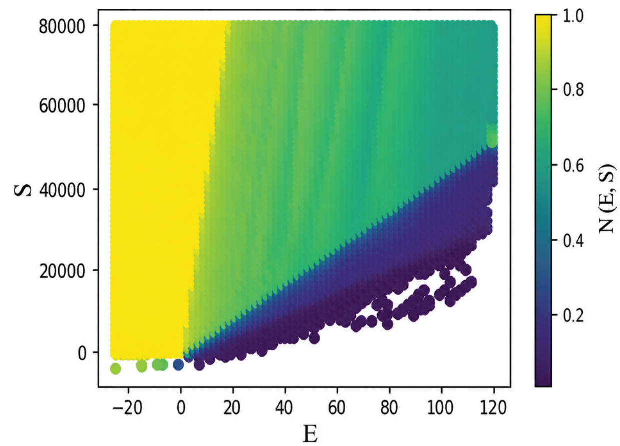

Figure 3. The relationship between the number of measurements $N(E,S)$ that is reduced and the exploratory and sensitivity parameters E and S, where the white space is when MAAPE values are greater than the predetermined error threshold *M*.

exploratory and sensitivity parameters E and S. Further details of determining the optimal values of E and S by employing a stochastic optimisation algorithm, the dual simulated annealing (DSA) and performing the training on a training dataset can be found in (Algabroun & Håkansson, 2025). The resulting optimal values of E and S are then implemented on a testing dataset to obtain a compressed signal of the original signal. The adaptively sampled (compressed) signal can then be reconstructed using interpolation with DSRA-PMLO and validated using the error metric MAAPE.

4.3. Applying DSRA-PMLO on the measured VVR signals

In the present study, DSRA-PMLO is implemented as an offline proof-of-concept to evaluate its suitability for vibration-based gravel road condition assessment. The optimisation of the algorithm parameters and the adaptive sampling are performed using fully recorded VVR signals, allowing the reconstructed signals to be compared directly with the original measurements. The objective is to determine whether adaptive sampling can reduce redundant data while preserving the diagnostic information required for condition assessment. Consequently, the present work does not address real-time adaptive acquisition, which requires causal sampling decisions based solely on previously acquired measurements.

DSRA-PMLO was applied to the VVR data from the test roads. The steps used for testing DSRA-PMLO on the simulated data were repeated with predetermined error thresholds *(M)* of 5%, 10%, 20%, 30%, 40% and 50% on the VVR data. The reductions in the sampled VVR data from each gravel road and for each *M* were recorded. The reduced VVR data were then reconstructed, and the reconstruction accuracy for each *M* was compared with the original signal using MAAPE. A moving average low-pass filtering technique was subsequently applied to the original and reconstructed squared VVR signals. Based on experience from previous work (Mbiyana & Kans, 2024; Mbiyana et al., 2024), averaging times ranging from 0 to 0.04 seconds were used to estimate the mean square value of the VVR as a function of time.

The original vehicle vibration records from each gravel road and the reconstructed signals for each *M* were then divided into eight adjacent frequency bands with the aid of band-pass filters. The squared magnitudes of the complex values of the VVR signals obtained were then scaled to provide the instantaneous power in each frequency sub-band. The findings from the original vehicle vibration signal obtained while driving on each gravel road and the reconstructed signals for each predetermined condition were compared.

5. Results

This section presents the results of testing DSRA-PMLO on simulated data (randomly generated signals), validating it using MAAPE and then applying DSRA-PMLO to the VVR signals obtained while driving on each gravel road. The resulting reduction in the sampling for each case is presented and discussed. The estimates of mean square values of the respective VVR signals are then presented, followed by the results of dividing the VVR signals into eight frequency sub-bands. Lastly, estimates of the mean values of the squared acceleration of the sub-band filtered VVR signals, as a function of the sub-band centre frequency, are presented for each scenario. The results from analysing the VVR signals before and after applying the DSRA-PMLO are compared to determine whether the same conclusions can be reached.

5.1. Dynamic sampling of the simulated random signals

Table 1 presents representative examples of the DSRA-PMLO algorithm's performance for the simulated data from the conducted comprehensive tests, with predetermined error thresholds ranging from 0.5% to 5%, reflecting different tolerance levels for approximation accuracy. The examples include three different test signals, each containing 120, 300 and 600 frequency components, with the frequencies randomly selected between 0 and 1200 Hz.

The representative examples of the error thresholds of 1% and 5% in Table 1 show the actual measured error (e_{MAAPE}) as we, as well as the difference between the measured error and the predetermined error threshold, and the percentage reduction in the samples. The results show that the difference between M and e_{MAAPE} ($\Delta eM = e_{MAAPE} - M$) is less than 0.5% for the test signals.

The reduction in the data samples shows a slight increase with an increase in the frequency components for $M = 1\%$. For $M = 5\%$, the reduction in the data samples is constant at 80% for all frequency components. These results indicate that the number of frequency components in the random signal has a negligible effect on the reduction in the data samples for a predetermined error threshold. The algorithm did not exceed the error threshold in some scenarios ($\boldsymbol{\Delta eM} < 0$), and it was slightly exceeded in others ($\boldsymbol{\Delta eM} > 0$). Nevertheless, the difference, $\boldsymbol{\Delta eM}$, remained consistent in all cases, staying below 0.5%, reflecting that the measured error closely matched the predetermined threshold.

5.2. Dynamic sampling and reconstruction of the VVR signal

DSRA-PMLO was applied to the VVR signals from the test roads with predetermined error thresholds (M) of 5%, 10%, 20%, 30%, 40% and 50%, respectively. Figure 4 shows the VVR collected from Road 1 and the reconstructed signal for an $M = 10\%$ for the first 100 samples.

After applying DSRA-PMLO, the VVR signal was approximated with 72% of the samples, resulting in a 28% reduction. The sampling rate varies based on changes in the VVR signal; i.e., the algorithm adapts according to signal variation. When there is a higher rate of change in the signal, a higher sampling rate is adopted. Conversely, a lower sampling rate is adopted when the rate of change is lower. Figure 5 shows the correlation between M and sample reduction for the VVR signals after applying DSRA-PMLO.

5.3. Estimates of the mean square acceleration of the VVR

The estimate of the mean square acceleration of the VVR signal and for the respective resampled and reconstructed signal are shown in Figure 6(a–c), respectively. From Figure 6, the estimates of the mean square acceleration show minimal deviation when compared to the estimated mean squared acceleration of

Table 1. Analysis of predetermined error threshold vs. measured error for the generated random signals with different frequency components and the respective reduction in the samples.

Predetermined error threshold, M	Number of frequency components	Measured error (e_{MAAPE})	$\Delta eM = e_{MAAPE} - M$	Reduction in samples (%)
$M = 1\%$	120	0.94	−0.06	62
	300	1.02	0.02	63
	600	1.04	0.04	64
$M = 5\%$	120	4.78	−0.22	80
	300	5.07	0.07	80
	600	5.15	0.15	80

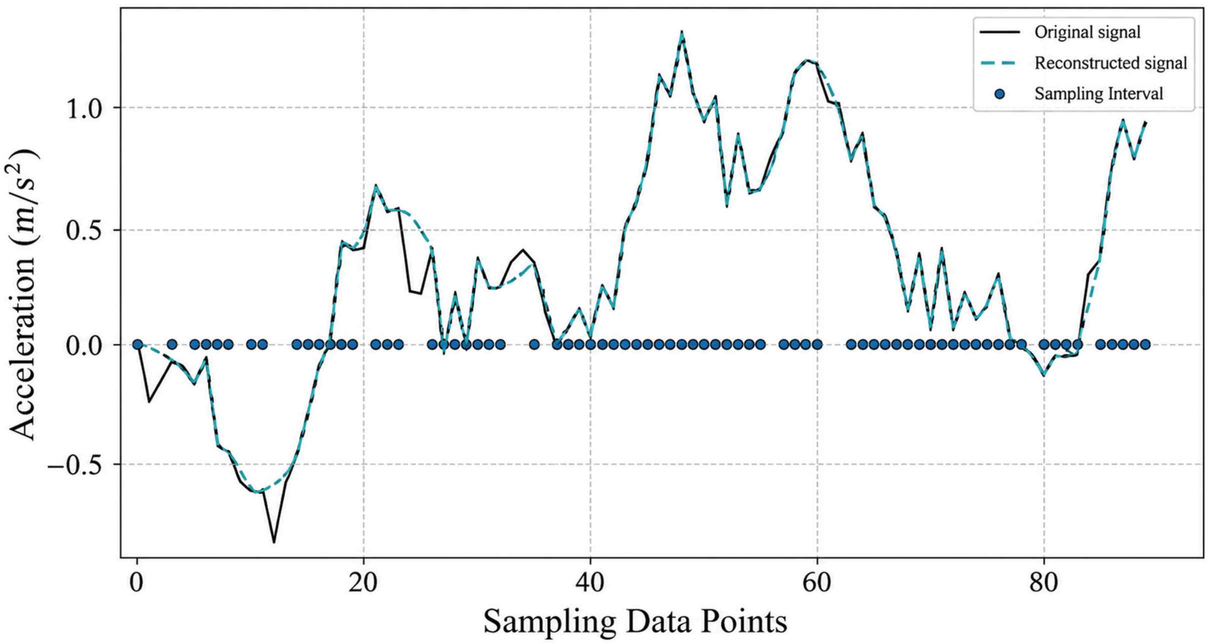

Figure 4. The vehicle vibration response (VVR) collected from road 1 and the reconstructed signal for a predetermined error threshold of 10% for the first 100 samples.

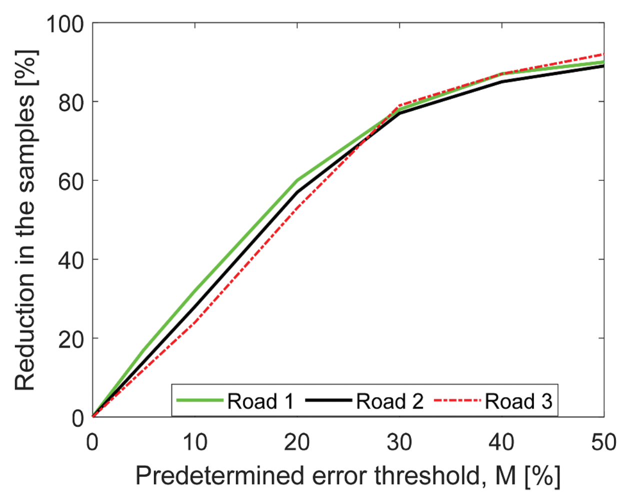

Figure 5. The correlation between the predetermined error threshold (*M*) and the reduction in samples for the test roads.

the original measured VVR signal, even with M up to 20%. With *M* equal to 20%, the samples are reduced by more than 50% for all three test roads (see Figure 5). Therefore, with only about 50% of the samples, the mean squared acceleration of the VVR signal can be estimated.

Moreover, increasing *M* above 20% results in a noticeable difference in the estimated mean-squared acceleration compared to the original measured vibration response signal. For instance, the mean squared acceleration is about 0.36 $\left(\frac{m}{s^2}\right)^2$ for the VVR from Road 1 when the $M = 0\%$, and it reduces to about 0.276 $\left(\frac{m}{s^2}\right)^2$ for $M = 50\%$; see Figure 6(a). A similar trend is observed for the VVR from Roads 2 and 3; see Figure 6(b,c).

Furthermore, by increasing *M*, the corresponding reduction in the samples for the VVR from Road 1, from 30% to 40%, is approximately 6%, and from 40% to 50% is approximately 14%; see Figure 5. The same observation is made for the VVR from Road 2 when *M* is greater than 20% and for the VVR from Road 3 when *M* is greater than 30%. Therefore, *M* greater than 30% for the VVR from Roads 1 and 3 and *M* greater

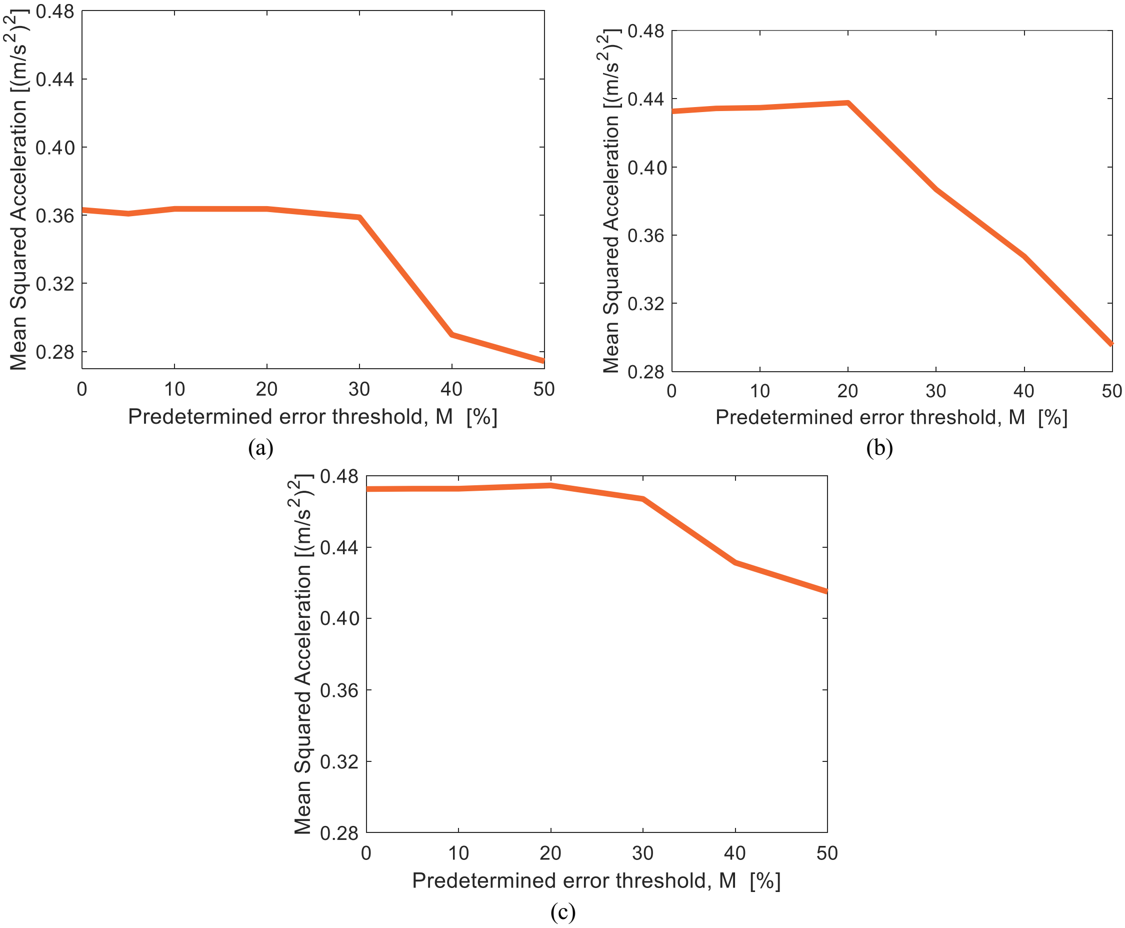

Figure 6. Estimates of the mean square acceleration of the VVR signal measured on (a) roads 1, (b) road 2 and (c) road 3, together with their dynamically sampled and reconstructed signal with predetermined error threshold M of 5%, 10%, 20%, 30%, 40% and 50%.

than 20% for the VVR from Road 2 is unjustified based on these differences in the estimated mean squared acceleration compared to the original measured vibration response signal.

5.4. Estimates of the mean square acceleration of the sub-band filtered vehicle vibration response

Based on experience from previous studies in (Mbiyana & Kans, 2024) and (Mbiyana et al., 2024), eight frequency sub-bands are sufficient for further analysis of the vehicle vibration responses, including the dynamically sampled and reconstructed signals. The averaging times used in this study are adopted from (Mbiyana & Kans, 2024) and (Mbiyana et al., 2024), as given in Table 2.

Estimates of the mean square value of the sub-band VVR signals were produced for the resampled and reconstructed signals at predetermined error thresholds (M) of 5%, 10%, 20%, 30%, 40%, and 50%, and then compared. Dividing the VVR signals into eight (8) adjacent sub-bands provides more information to detect faults by analysing the behaviour of the signals in the respective adjacent frequency bands.

5.5. The sub-band filtered VVR signals for estimating the mean square acceleration

The VVR signals were divided into eight (8) adjacent sub-bands. The signal behaviours were compared for the different scenarios, i.e., the measured VVR signals, with those of their respective dynamically sampled and reconstructed signals. The sub-band VVR signals measured on Road 1, along with the respective dynamically sampled and reconstructed signals with M values of 5%, 10%, 20%, 30%, 40%, and 50%, are shown in Figure 7.

Table 2. Averaging time for the moving average on the vibration response divided into eight adjacent frequency bands.

		Averaging time for the eight sub-bands (s)		
Frequency sub-band	Normalised centre frequencies f_k (Hz)	Road 1	Road 2	Road 3
1	0	0.02	0.03	0.03
2	128	0.01	0.02	0.03
3	256	0.005	0.01	0.0025
4	384	0.001	0.001	0.0005
5	512	0.0005	0.001	0.0005
6	640	0.0025	0.0005	0.0025
7	768	0.01	0.0005	0.0075
8	896	0.005	0.0005	0.005

The squared magnitude of the sub-band filtered VVR signals measured on gravel Road 1 and the resampled and reconstructed signals with M of 5%, 10%, 20% and 30% in Figure 7 show similarities in the signal pattern in their respective frequency bands. As M exceeds 30%, the sub-band VVR signals exhibit variations compared to the measured signal, particularly in the higher-frequency sub-bands.

For instance, in the 896 Hz frequency subband for M of 40% and 50%, respectively (see Figure 7((f,g)), there is a noticeable variation in the signal compared to the measured signal in Figure 7(a). The response at approximately 280s is $4.5\left(\frac{m}{s^2}\right)^2$ in the 896 Hz frequency subband in Figure 7(a) and reduces to approximately $2.98\left(\frac{m}{s^2}\right)^2$ for $M = 40\%$ Figure 7(f) and is almost zero for $M = 50\%$ Figure 7(g). Similar results were obtained for VVR signals from Roads 2 and 3. As the error threshold M exceeds 20%, the reconstructed sub-band vehicle vibration signals deviate significantly from the measured signals, especially in the higher-frequency sub-bands. According to (Mbiyana & Kans, 2024; Mbiyana et al., 2024), the VVR in the higher frequency bands is associated with the gravel road's general homogeneity. The higher frequency bands were primarily associated with the loose gravel on the road surface.

5.6. Estimates of the mean square acceleration of the sub-band filtered VVR measured on roads 1, 2 and 3

Figure 8(a) shows that as M increases and exceeds 30%, the estimated mean values of the squared acceleration for the higher frequency bands of the vehicle's vibration response begin to deviate more from Road 1, as also observed in Figure 7, particularly in the higher frequency bands. The findings suggest that gravel road faults linked to the lower frequency sub-band can be evaluated using a higher M than faults linked to the higher frequency sub-band. According to (Mbiyana & Kans, 2024; Mbiyana et al., 2024), the vehicle's vibration response in the lower frequency bands is associated with irregularities in the gravel road, such as potholes and corrugations, which trigger the vehicle's vibrations. Therefore, the estimated mean values of the squared acceleration of the sub-band VVR from gravel Road 1 can be approximated with M of up to 30% for all the adjacent frequency sub-bands.

From Figure 8(b), as M is increased, the estimated mean values of the squared acceleration of the sub-band VVR in the higher frequency bands for M greater than 20% deviate from the estimated mean values of the VVR from Road 2, as observed also for the VVR from Road 1. These results indicate that the VVR signal measured on gravel Road 2 can be approximated with M of up to 20% for all the adjacent frequency sub-bands. Generally, Road 2 had less loose gravel on the road surface, which is detected in the higher frequency bands. The mean squared acceleration for $M = 30\%$, 40% and 50% deviates from the mean squared acceleration of the measured VVR in the higher frequency bands.

In Figure 8(c), the estimated mean values of the squared acceleration of the sub-band VVR indicate that the VVR signal measured on gravel Road 3 can be approximated with M of up to 20% for all the adjacent frequency sub-bands. As M increases, as shown in Figure 8(c), the estimated mean values of the squared acceleration of the sub-band VVR in the higher frequency bands for M greater than 20% deviate from the estimated mean values of the VVR from Road 3. Road 3 generally had more loose gravel on the road surface than Roads 1 and 2, which excited the vehicle's vibration response in the higher frequency bands. In Figure 8(c), the mean squared acceleration for $M = 30\%$, 40%, and 50% deviates from the mean squared acceleration of the measured VVR in the higher frequency bands.

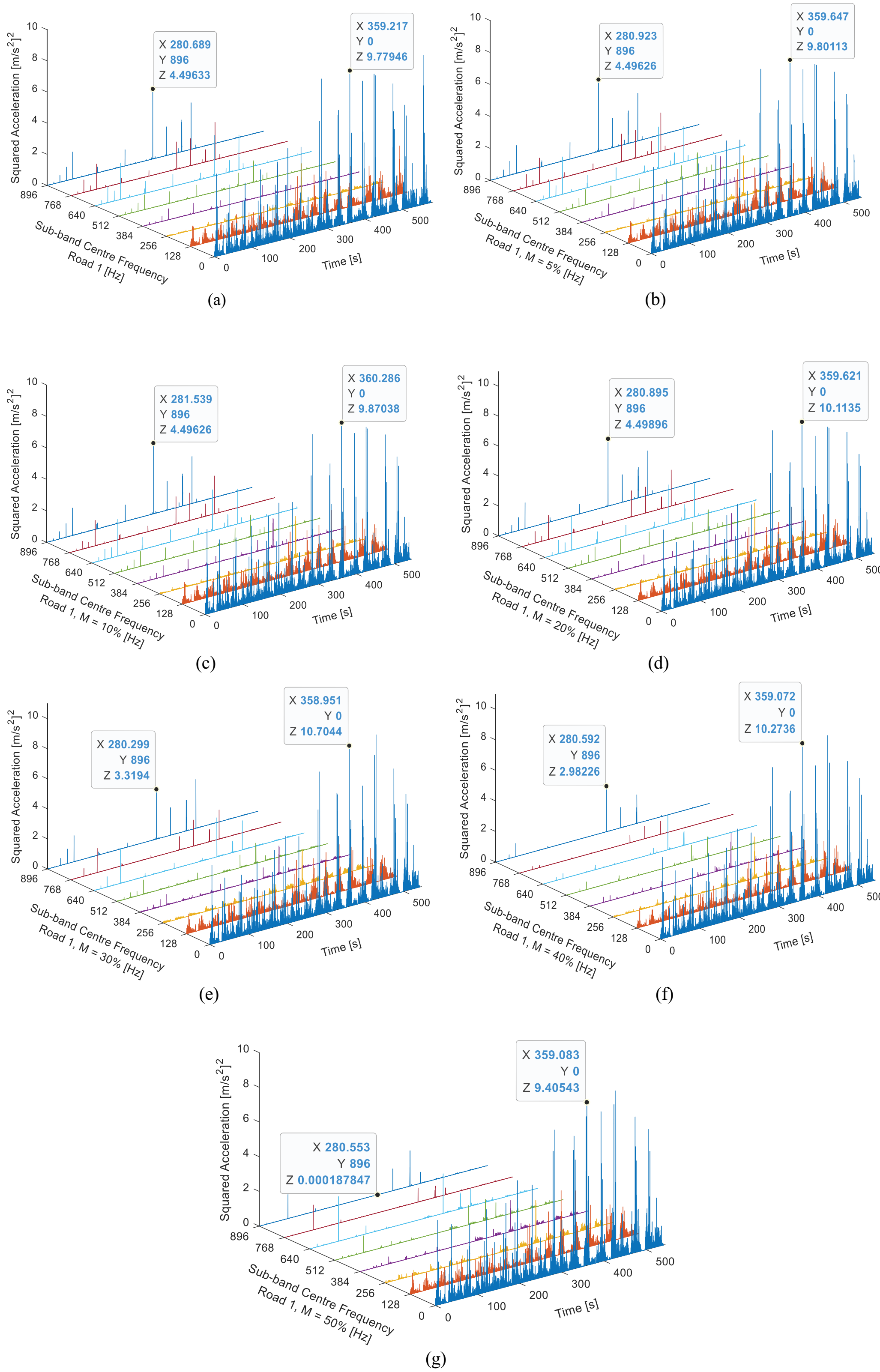

Figure 7. The vehicle vibration response (VVR) signals divided into eight (8) sub-bands, and the averaging times given in Table 2 as a function of time and used to estimate the mean square value (a) measured with the IEPE accelerometer on gravel road 1, while (b), (c), (d), (e), (f), and (g) are the resampled and reconstructed signals with predetermined error threshold *M* of 5%, 10%, 20%, 30%, 40% and 50%.

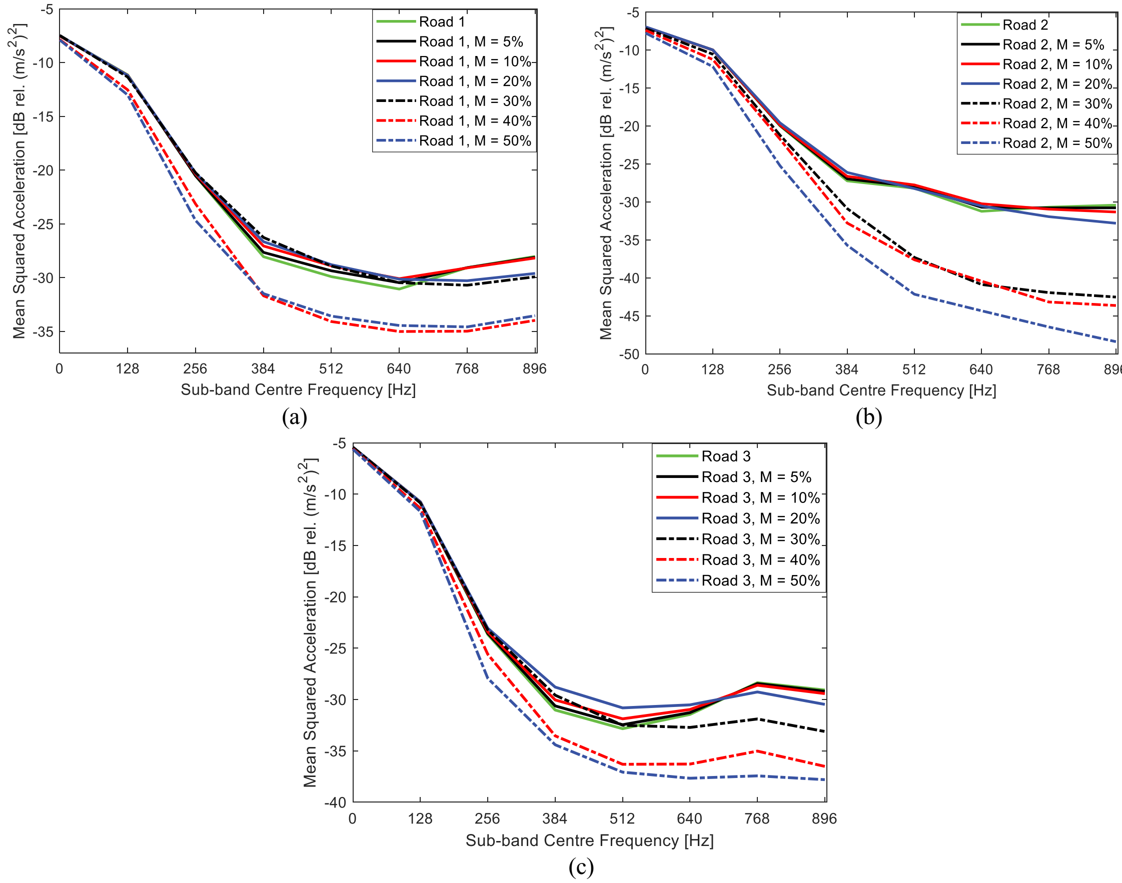

Figure 8. Estimates of mean values of the squared acceleration of the sub-band filtered vehicle vibration response (VVR) from gravel (a) road 1, (b) road 2 and (c) road 3 for each sub-band centre frequency in decibel scale.

6. Performance evaluation of the dynamic sampling rate algorithm – Parametric machine learning optimisation

Unlike previous studies that evaluated DSRA-PMLO primarily for environmental and IoT sensing applications (Algabroun & Håkansson, 2025), this study demonstrates its applicability to vibration-based gravel road condition assessment. Vehicle vibration response (VVR) signals exhibit unique characteristics, including frequency band content, transient impacts caused by potholes and corrugations, and the need to preserve spectral information for reliable condition assessment. The results show that DSRA-PMLO preserves these characteristics while substantially reducing redundant data. It should be noted that the present implementation represents an offline proof-of-concept rather than a real-time adaptive acquisition strategy. The complete VVR signals were available during optimisation and validation to enable direct comparison between the original and dynamically sampled signals. This approach provides a controlled environment for evaluating whether DSRA-PMLO preserves the information required for gravel road condition assessment before considering real-time deployment.

For Road 1, a predetermined error threshold of 30% reduced the number of samples by 77% while still enabling the detection and identification of gravel road faults. Similarly, for Roads 2 and 3, predetermined error thresholds of 20% reduced the samples by approximately 53% and 57%, respectively, without compromising fault detection. However, considering all three test roads and the preservation of vibration characteristics, a predetermined error threshold of 20% provides the best balance between data reduction and condition assessment accuracy. At this threshold, more than 50% of the VVR data can be eliminated while preserving the information required to detect and identify gravel road faults, thereby extending the applicability of DSRA-PMLO to intelligent gravel road condition assessment and monitoring systems.

Table 3. Comparison of the predetermined error threshold M and the measured error (e_{MAAPE}), including the reduction in sample data for the test gravel roads.

Gravel Road	Predetermined error threshold M (%)	Measured error (e_{MAAPE})	$\Delta eM = e_{MAAPE} - M$	Reduction in samples (%)
Road 1	5	5.31	0.31	17
	10	10.01	0.01	32
	20	20.00	0.00	60
	30	30.00	0.00	78
	40	40.00	0.00	87
	50	50.00	0.00	90
Road 2	5	4.54	−0.45	12
	10	10.00	0.00	24
	20	20.00	0.00	53
	30	30.00	0.00	79
	40	40.00	0.00	87
	50	50.00	0.00	92
Road 3	5	4.73	−0.27	14
	10	10.00	0.00	28
	20	20.00	0.00	57
	30	30.00	0.00	78
	40	40.00	0.00	85
	50	50.00	0.00	89

Table 3 compares the predetermined error threshold M and the measured error (e_{MAAPE}) from the VVR signals collected while driving on gravel roads 1, 2 and 3. The difference between $Mande_{MAAPE}$, i.e., ΔeM, was less than 0.5% for all cases. The algorithm slightly exceeded the error threshold in some scenarios, specifically for gravel Road 1, and the predetermined error thresholds of 5% and 10%. It remained within the error threshold for all the other remaining scenarios. Nevertheless, the difference, $\boldsymbol{\Delta eM}$, remained consistent in all cases, staying below 0.5%, reflecting that the measured error closely matched the predetermined threshold.

6.1. Checking for aliasing distortions using the power spectral density estimate

The PSD estimate of the resampled and reconstructed VVR signals for the VVR from gravel Road 3 is presented in Figure 9. This analysis was conducted to check for signal distortion after dynamic sampling with DSRA-PMLO. Road 3 was selected for this analysis because it was significantly worse than Roads 1 and 2, with numerous potholes and loose gravel scattered throughout the entire road section. Signal distortions would be more detectable on a gravel road that is in poor condition when the VVR signal is dynamically sampled with DSRA-PMLO at a higher predetermined error threshold.

Figure 9 shows the PSD estimate comparisons. As the predetermined error threshold increases, the resampled signals noticeably deviate from the original signal, indicating distortion. For the 20% error threshold, see Figure 9(c); the resampled and reconstructed VVR signal begins to deviate from the original signal around 180 Hz. These deviations become even more pronounced for error thresholds of 30%, 40%, and 50%. Additionally, the power of the resampled and reconstructed signals (represented by the area under the PSD estimate) is lower compared to the original signal:

- For error thresholds of 30% and 40%, the power is lower than the original signal from approximately 150 Hz to the highest frequency.
- For the 50% error threshold, the power is lower from around 100 Hz to the highest frequency.

These distortions in vehicle vibration signals can lead to inaccurate interpretations, underestimating fault severity, and misclassifying the condition of gravel roads. Surface irregularities, such as loose gravel, corrugations, and potholes, may be misrepresented. For instance, the severity and extent of loose gravel, which is associated with higher frequencies, would be misinterpreted for error thresholds of 30%, 40%, and 50%. The resampled signals do not retain the significant frequency components for higher error thresholds. To avoid such distortions and inaccurate interpretations, the dynamic sampling rate of the DSRA-PMLO must be sufficiently high, which is achieved by setting a lower predetermined error threshold. Aliasing in the resampled and reconstructed VVR signals is a possibility. Higher frequency

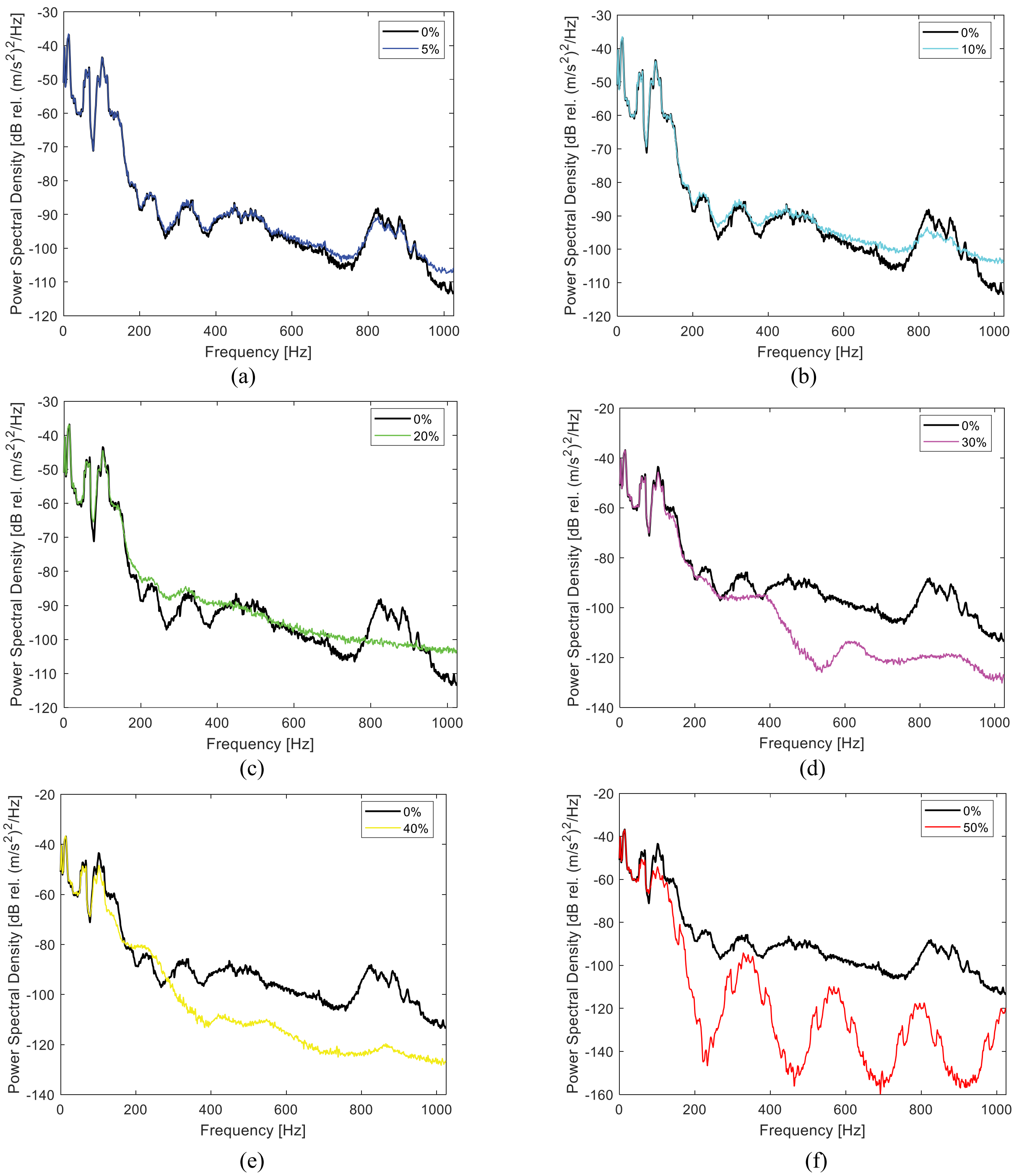

Figure 9. Power spectral density estimates of the vehicle vibration signal collected from gravel road 3 to compare the original and resampled signals after dynamic sampling with DSRA-PMLO and predetermined error threshold (a) 5%, (b) 10%, (c) 20%, (d) 30%, (e) 40% and (f) 50%.

components could have been misinterpreted as lower frequencies after resampling, as seen by the presence of higher peaks in the lower frequencies at error thresholds of 30%, 40%, and 50%, see Figure 9(c–f) for frequencies lower than 50 Hz. This study does not go into detail to investigate the extent of aliasing. Similar results were observed for gravel Roads 1 and 2, although not as pronounced as for gravel Road 3 (see Figure 10).

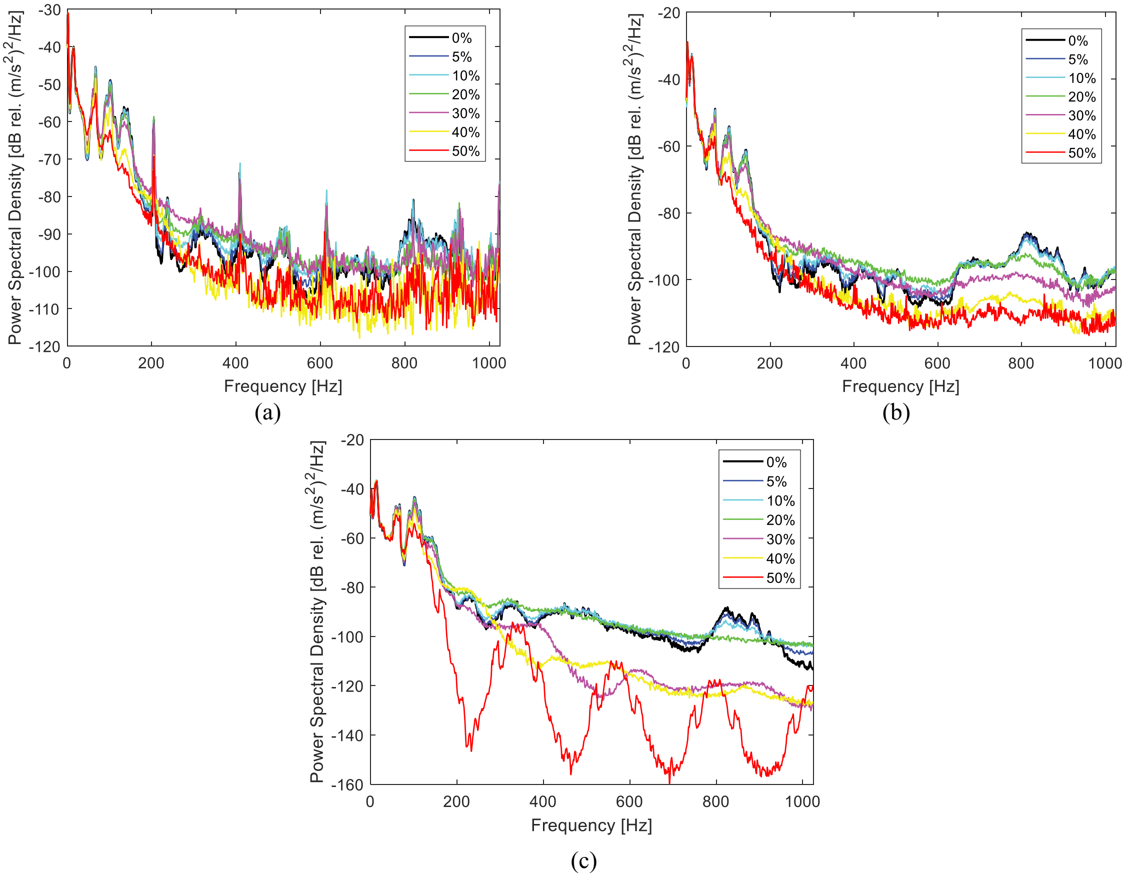

Figure 10. Power spectral density estimates of the vehicle vibration signal to compare the original and resampled signals after dynamic sampling with DSRA-PMLO and predetermined error thresholds of 5%, 10%, 20%, 30%, 40% and 50% collected from (a) gravel road 1, (b) gravel road 2 and (c) gravel road 3.

7. Conclusion and future works

Rather than introducing a new adaptive sampling algorithm, the study validates an application-oriented framework for evaluating adaptive sampling of vehicle vibration response signals. This study demonstrates that the developed DSRA-PMLO and proposed by Algabroun and Håkansson (Algabroun & Håkansson, 2025) can be successfully adapted for vibration-based gravel road condition assessment and significantly enhances the efficiency of condition data collection and processing for gravel road assessment by dynamically adjusting the sampling interval in response to variations in the VVR signal trends. By employing this adaptive sampling technique, redundant data are minimised while maintaining high accuracy in condition assessments. Experimental results show that DSRA-PMLO preserves the diagnostic information required for gravel road condition assessment while reducing data volume by more than 50% when an approximation-error threshold of 20% is adopted and the results remained consistent with those obtained using the entire dataset. Gravel road faults, such as potholes, corrugations, and loose gravel, were not only identified but also differentiated, allowing for insights into their time-varying properties from the resampled signals. The faults were detected by dividing the vibration signals into eight adjacent frequency bands and estimating the mean-square value of each sub-band signal.

The study demonstrates that an error threshold of up to 20% provides an optimal trade-off between data reduction and accuracy in gravel road condition assessment using the DSRA-PMLO. At this level, the mean-square value estimates closely match those from the original signals. However, thresholds beyond 20% result in pronounced distortions and aliasing, as revealed by comparing the Power Spectral Density estimates, compromising fault detection reliability. Therefore, applying adaptive sampling techniques, such as DSRA-PMLO, to reduce redundant data is promising for efficient collection and storage of condition data. The stored condition data can subsequently be used to assess and classify the condition of the gravel roads. By removing unnecessary data, DSRA-PMLO directly contributes to broader infrastructure sustainability goals in gravel road maintenance through efficient data transmission, reducing storage demands and energy consumption while lowering the carbon footprint and environmental impact. Gravel road condition data sampling using the DSRA-PMLO shows potential for real-time condition monitoring deployment, including the integration of commercial vehicle fleets in a participatory, data-driven approach to road condition assessment using smartphones or embedded sensors.

Future work will build on this established reference and extend this offline proof-of-concept towards a real-time implementation of DSRA-PMLO for participatory gravel road monitoring. This will require the development of a causal adaptive sampling strategy capable of making sampling decisions using only previously acquired measurements while ensuring that transient events, such as pothole impacts and corrugations, are reliably captured. The performance of the real-time implementation will be validated using smartphone accelerometers, radar sensors, and participatory data collected from commercial vehicle fleets. Future work will also include a comparative evaluation of the performance of DSRA-PMLO against conventional fixed-rate sampling, uniform downsampling, and representative signal compression techniques and compare their relative effectiveness for vibration-based gravel road condition assessment. Additionally, future works will investigate the application of a participatory data-driven approach, particularly its potential deployment with commercial vehicle fleets, incorporating dynamic sampling and signal reconstruction to enhance gravel road condition assessment. A comprehensive analysis of the effects of aliasing and signal distortion resulting from interpolation, especially at high frequencies due to dynamic sampling with predetermined error thresholds, will also be conducted. Furthermore, the algorithm requires validation across diverse environmental and geographical contexts, leveraging participatory or crowdsourced data collection platforms.

Author contributions

CRediT: **Keegan Mbiyana:** Conceptualization, Data curation, Formal analysis, Investigation, Methodology, Project administration, Software, Validation, Visualization, Writing – original draft, Writing – review & editing; **Hatem Algabroun:** Conceptualization, Formal analysis, Investigation, Methodology, Software, Validation, Visualization, Writing – original draft, Writing – review & editing; **Maxime Riou:** Data curation, Formal analysis, Investigation, Software, Visualization; **Mirka Kans:** Conceptualization, Data curation, Formal analysis, Investigation, Methodology, Software, Supervision, Validation, Visualization, Writing – original draft, Writing – review & editing; **Rammohan Kodakadath Premachandran:** Data curation, Formal analysis, Investigation, Software, Visualization; **Lars Håkansson:** Conceptualization, Formal analysis, Investigation, Supervision, Validation, Visualization, Writing – original draft, Writing – review & editing.

Disclosure statement

No potential conflict of interest was reported by the author(s).

Notes on contributors

Keegan Mbiyana is a researcher with interests in data-driven maintenance, condition monitoring, and infrastructure asset management. His work develops objective methods for gravel road condition assessment using vehicle vibration response, sensor technologies, classical signal processing techniques and machine learning. He has experience in maintenance engineering and asset management across the public and private sectors.

Hatem Algabroun is a Senior Lecturer at the Mechanical Engineering, Linnaeus University, Sweden. His research focuses on smart maintenance, predictive maintenance, condition monitoring, adaptive sampling, and the digitalisation of industrial systems. He conducts research on intelligent maintenance solutions to improve the reliability and efficiency of manufacturing and infrastructure systems.

Maxime Riou completed a Master's degree in Computer Engineering at EPITA: School of Computer Engineering, Paris, France. He undertook a research internship at Linnaeus University, Sweden, where he worked on machine learning, data-driven approaches for gravel road condition assessment and adaptive sampling techniques.

Mirka Kans is an Associate Professor of Mechanical Engineering at Linnaeus University, Sweden, and an Associate Professor in the Department of Technology Management and Economics at Chalmers University of Technology, Gothenburg, Sweden. Her research focuses on maintenance and infrastructure asset management, digital transformation, industrial information systems, and data-driven decision support for sustainable maintenance, with recent work also addressing circular production, remanufacturing, and Industry 4.0/5.0 in manufacturing and infrastructure systems.

Rammohan Kodakadath Premachandran is a researcher in Mechanical Engineering. His research focuses on signal processing, condition monitoring, vibration analysis, and simulation of mechanical systems, with applications in drilling systems, manufacturing processes, and infrastructure and mechanical equipment condition monitoring.

Lars Håkansson is Professor whose research focuses on signal analysis, condition monitoring, signal processing, active noise and vibration control, and analytical and experimental modelling of mechanical and acoustic systems. He is a Fellow of the International Institute of Acoustics and Vibration (IIAV) and an Associate Editor of the International Journal of Acoustics and Vibration.

ORCID

Keegan Mbiyana http://orcid.org/0000-0003-2619-9137

References

Ahmed, K. M. U., Bollen, M. H. J., & Alvarez, M. (2021). A review of data centers energy consumption and reliability modeling. *IEEE Access*, *9*, 152536–152563. https://doi.org/10.1109/ACCESS.2021.3125092

Albatayneh, O., Forslöf, L., & Ksaibati, K. (2019). Developing and validating an image processing algorithm for evaluating gravel road dust. *International Journal of Pavement Research and Technology*, *12*(3), 288–296. https://doi.org/10.1007/s42947-019-0035-y

Aleadelat, W., & Ksaibati, K. (2018). A comprehensive approach for quantifying environmental costs associated with unpaved roads dust. *Journal of Environmental Economics and Policy*, *7*(2), 130–144. https://doi.org/10.1080/21606544.2017.1374214

Algabroun, H. (2020). Dynamic sampling rate algorithm (DSRA) implemented in self-adaptive software architecture: A way to reduce the energy consumption of wireless sensors through event-based sampling. *Microsystem Technologies*, *26*(4), 1067–1074. https://doi.org/10.1007/s00542-019-04631-9

Algabroun, H., & Håkansson, L. (2025). Parametric machine learning - based adaptive sampling algorithm for efficient IoT data collection in environmental monitoring. *Journal of Network and Systems Management*, *33*(5). https://doi.org/10.1007/s10922-024-09881-1

Alippi, C., Anastasi, G., DiFrancesco, M., & Roveri, M. (2010). An adaptive sampling algorithm for effective energy management in wireless sensor networks with energy-hungry sensors. *IEEE Transactions on Instrumentation and Measurement*, *59*(2), 335–344. https://doi.org/10.1109/TIM.2009.2023818

Alzubaidi, H., & Magnusson, R. (2002). Deterioration and rating of gravel roads: State of the art. *Road Materials and Pavement Design*, *3*(3), 235–260. https://doi.org/10.1080/14680629.2002.9689924

Andrén, L., Håkansson, L., Brandt, A., & Claesson, I. (2004). Identification of dynamic properties of boring bar vibrations in a continuous boring operation. *Mech Syst Signal Process*, *18*(4), 869–901. https://doi.org/10.1016/S0888-3270(03)00093-1

Bardal, K. G., & Jørgensen, F. (2017). Valuing the risk and social costs of road traffic accidents - seasonal variation and the significance of delay costs. *Transport Policy*, *57*, 10–19. https://doi.org/10.1016/j.tranpol.2017.03.015

Ben-Aboud, Y., Licea, D. B., Ghogho, M., & Kobbane, A. (2021). On adaptive sampling algorithms for IoT devices. In *ICC, 2021 - IEEE international conference on communications* (pp. 1–7). IEEE.

Bendat, J. S., & Piersol, A. G. (2012). *Random data. Analysis and measurement procedures* (4th ed.). John Wiley and Sons.

Chu, D., Deshpande, A., Hellerstein, J. M., & Hong, W. (2006). Approximate data collection in sensor networks using probabilistic models. In *22nd IEEE International Conference on Data Engineering (ICDE 2006)*. IEEE Computer Society. https://doi.org/10.1109/ICDE.2006.21

Daniel, P., Lucas, M., André, D., & Courret, G. (2021). Adaptive resampling for data compression. *Array*, *12*, 2021. https://doi.org/10.1016/j.array.2021.100076

Davis, M. S., & Lanterman, A. D. (2015). Aliasing in recurrently sampled signals with an application to synthetic aperture imaging. *IEEE Transactions on Signal Processing*, *63*(12), 3088–3095. https://doi.org/10.1109/TSP.2015.2417503

Edvardsson, K., Lundberg, T., & Sjögren, L. (2015). Objektiv mätmetod för tillståndsbedömning av grusväglag. Rapport 863. The Swedish National Road and Transport Research Institute (VTI).

Gindullina, E., Badia, L., & Vilajosana, X. (2020). Energy modeling and adaptive sampling algorithms for energy-harvesting powered nodes with sampling rate limitations. *Transactions on Emerging Telecommunications Technologies*, *31*(3), 1–15. https://doi.org/10.1002/ett.3754

Giouroukis, D., Dadiani, A., Traub, J., Zeuch, S., & Markl, V. (2020). A survey of adaptive sampling and filtering algorithms for the internet of things. In J. Gascon-Samson, K. Zhang, K. Daudjee, & B. Kemme (Eds.), *Proc. 14th ACM International conference on distributed and event-based Systems (DEBS' 20)* (pp. 27–38). Association for Computing Machinery (ACM). https://doi.org/10.1145/3401025.3403777

Gorges, C., Öztürk, K., & Liebich, R. (2019). Impact detection using a machine learning approach and experimental road roughness classification. *Mechanical Systems and Signal Processing*, *117*, 738–756. https://doi.org/10.1016/j.ymssp.2018.07.043

Hong Pham, S. V., Tien Nguyen, K. V., Quang Le, H., & Tran, P. L. H. (2024). Road surface damages allocation with RTI-IMS software based on YOLO V5 model. *Sustainable and Resilient Infrastructure*, *9*(3), 242–261. https://doi.org/10.1080/23789689.2023.2287857

Hurtig, P., Larsson, P., Lindholm, M., Rizzi, M., Sternlund, S., Elmqvist, A. L., Fredriksson, R., Forsman, Å., Vadeby, A., & Amin, K. (2023). Trafikverkets publikationer 2023:116. Trafikverket (Swedish Transport Administration). http://urn.kb.se/resolve?urn:nbn:se:trafikverket:diva-12242

International Transport Forum. (2021). *Road safety report*. https://www.itf-oecd.org/sites/default/files/sweden-road-safety.pdf

Kans, M., Campos, J., & Håkansson, L. (2020). Current practices and new approaches within condition monitoring of gravel roads. *International Journal of COMADEM*, *23*(4), 3–8.

Kim, H., Ahn, C. R., & Yang, K. (2016). A people-centric sensing approach to detecting sidewalk defects. *Advanced Engineering Informatics*, *30*(4), 660–671. https://doi.org/10.1016/j.aei.2016.09.001

Kim, S., & Kim, H. (2016). A new metric of absolute percentage error for intermittent demand forecasts. *International Journal of Forecasting*, *32*(3), 669–679. https://doi.org/10.1016/j.ijforecast.2015.12.003

Levinzon, F. (2015). *Piezo-electric accelerometers with integral electronics*. Springer International Publishing.

Liu, G. R., Dai, K. Y., & Lim, K. M. (2004). Static and vibration control of composite laminates integrated with piezo-electric sensors and actuators using the radial point interpolation method. *Smart Materials & Structures*, *13*(6), 1438–1447. https://doi.org/10.1088/0964-1726/13/6/015

Liu, W., Wang, R., Ding, R., Meng, X., & Yang, L. (2020). On-line estimation of road profile in semi-active suspension based on unsprung mass acceleration. *Mechanical Systems and Signal Processing*, *135*, 106370. https://doi.org/10.1016/j.ymssp.2019.106370

Loprencipe, G., & Zoccali, P. (2017). Ride quality due to road surface irregularities: Comparison of different methods applied on a set of real road profiles. *Coatings*, *7*(5), 59. https://doi.org/10.3390/coatings7050059

Lu, T., Liu, G., Li, W., Chang, S., & Guo, W. (2017). Distributed sampling rate allocation for data quality maximisation in rechargeable sensor networks. *Journal of Network and Computer Applications*, *80*, 1–9. https://doi.org/10.1016/j.jnca.2016.12.021

Luo, C., Wu, F., Sun, J., & Chen, C. W. (2009). Compressive data gathering for large-scale wireless sensor networks. In K. G. Shin, Y. Zhang, R. Bagrodia, and R. Govindan (Eds.), *Proc. 15th annual international conference on Mobile computing and networking (MOBICOM)* (pp. 145–156). Association for Computing Machinery (ACM). https://doi.org/10.1145/1614320.1614337

Mbiyana, K., & Kans, M. (2024). A comparative study regarding information quality of data acquisition methods for gravel road condition measurement. In G. Abdul-Nour, M. Ngoc Dinh, T. Seecharan, A. Crespo Márquez, D. Komljenovic, J. Amadi-Echendu, & J. Mathew (Eds.), *Proc. 17th WCEAM - Sustainable management of engineered assets in a post-COVID-19 world: Industry 4.0, digital transformation, society 5.0 and beyond, part of the book series: Lecture notes in mechanical engineering* (pp. 343–355). Springer Nature Switzerland AG. https://doi.org/10.1007/978-3-031-59042-9_28

Mbiyana, K., & Kans, M. (2024). A participatory data-driven approach for unpaved road condition monitoring. *Journal of Construction Project Management and Innovation*, *14*(1), 57–71. https://doi.org/10.36615/wmwdwh65

Mbiyana, K., Kans, M., & Campos, J. (2021). A data-driven approach for gravel road maintenance. In G. Chattopadhyay (Ed.), *International conference on maintenance and intelligent asset management (ICMIAM)* (pp. 1–6). IEEE. https://doi.org/10.1109/ICMIAM54662.2021.9715196

Mbiyana, K., Kans, M., Campos, J., & Håkansson, L. (2022). Literature review on gravel road maintenance: Current state and directions for future research. *Transportation Research Record*, *2677*(5), 506–522. https://doi.org/10.1177/03611981221133102

Mbiyana, K., Kans, M., Premachandran, R. K., & Håkansson, L. (2024). Assessing corrugations and the influence of vehicle speed: A vehicle vibration response approach to gravel road condition assessment. In W. van Keulen & J. Kok (Eds.), *Proc. 30th international congress on sound and vibration (ICSV30)* (pp. 1–8). Society of Acoustics. https://iiav.org/content/archives_icsv_last/2024_icsv30/content/papers/papers/full_paper_188_20240422162748902.pdf

Nižetić, S., Šolić, P., López-de-Ipiña González-de-Artaza, D., & Patrono L. (2020). Internet of things (IoT): Opportunities, issues and challenges towards a smart and sustainable future. *Journal of Cleaner Production*, *274*, 2020. https://doi.org/10.1016/j.jclepro.2020.122877

Ntakpe, J. L., Gillich, G. R., Minda, A. A., Mituletu, I. C., & Gillich, N. (2017). Two-stage interpolation algorithm for precise frequency estimation of vibration signals. *Romanian Journal of Acoustics and Vibration*, *14*(2), 125–130.

Nunes, D. E., & Mota, V. F. S. (2019). A participatory sensing framework to classify road surface quality. *Journal of Internet Services and Applications*, *10*(1), 1–16. https://doi.org/10.1186/s13174-019-0111-1

Padhy, P., Dash, R. K., Martinez, K., & Jennings, N. R. (2006). A utility-based sensing and communication model for a glacial sensor network. In H. Nakashima, M. P. Wellman, G. Weiss, & P. Stone (Eds.), *Proc. 5th International joint conference on autonomous agents and multiagent systems* (pp. 1353–1360). Association for Computing Machinery (ACM). https://doi.org/10.1145/1160633.1160885

Pampolina, M., Onayev, A., Therrien, M., & Swei, O. (2024). A network-level management system to mitigate the global warming potential of road pavements. *Sustainable and Resilient Infrastructure*, *9*(1), 49–62. https://doi.org/10.1080/23789689.2023.2253411

Papoulis, A., & Pillai, S. U. (2002). *Probability random variables, and stochastic processes* (4th ed.). McGraw-Hill.

Rafiei, A., Abdi Kordani, A., Zarei, M., & Hosseinian, S. M. (2025). Simulation and modeling of roadways containing rutting damage in horizontal curves: A safety study using lateral friction coefficient. *Sustainable and Resilient Infrastructure*, *10*(4), 385–406. https://doi.org/10.1080/23789689.2025.2454186

Rana, S., & Asaduzzaman, A. (2021). Vibration based pavement roughness monitoring system using vehicle dynamics and smartphone with estimated vehicle parameters. *Results in Engineering*, *12*, 100294. https://doi.org/10.1016/j.rineng.2021.100294

Rault, T., Abdelmadjid, B., & Challal, Y. (2014). Energy efficiency in wireless sensor networks: A top-down survey. *Computer Networks*, *67*, 104–122. https://doi.org/10.1016/j.comnet.2014.03.027

Rodriguez-Pabon, C., Riva, G., Zerbini, C., Ruiz-Rosero, J., Ramirez-Gonzalez, G., & Corrales, J. C. (2022). An adaptive sampling period approach for management of IoT energy consumption: Case study approach. *Sensors*, *22*(4), 1472. https://doi.org/10.3390/s22041472

Shtayat, A., Moridpour, S., Best, B., & Abuhassan, M. (2023). Using supervised machine learning algorithms in pavement degradation monitoring. *International Journal of Transportation Science and Technology*, *12*(2), 628–639. https://doi.org/10.1016/j.ijtst.2022.10.001

Shtayat, A., Moridpour, S., Best, B., & Daoud, H. (2023). Application of noise-cancelling and smoothing techniques in road pavement vibration monitoring data. *International Journal of Transportation Science and Technology*, *14*, 110–119. https://doi.org/10.1016/j.ijtst.2023.04.002

Swedish Civil Contingencies Agency. (2012). *Social costs of accidents in Sweden*. (MSB 340–11). MSB - Swedish Civil Contingencies Agency.

Swedish Transport Agency. (2014). *Bedömning av grusväglag*. vol. TDOK 2014: Version 1.0, 0–12.

Vaidyanathan, P. (1993). *Multirate systems and filter banks*. Prentice Hall Signal Processing Series.

Wang, W., Zhou, S., & Yang, Q. (2022). A characterisation method for pavement structural condition assessment based on the distribution parameter of the vehicle vibration signal. *Applied Sciences*, *12*(2), 683. https://doi.org/10.3390/app12020683

Welch, P. D. (1967). The use of fast Fourier transform for the estimation of power spectra: A method based on time averaging over short, modified periodograms. *IEEE Transactions on Audio and Electroacoustics*, *15*(2), 70–73. https://doi.org/10.1109/TAU.1967.1161901

Yu, Q., Fang, Y., & Wix, R. (2022). Pavement roughness index estimation and anomaly detection using smartphones. *Automation in Construction*, *141*, 104409. https://doi.org/10.1016/j.autcon.2022.104409

Žuraulis, V., Sivilevičius, H., Šabanovič, E., Ivanov, V., & Skrickij, V. (2021). Variability of gravel pavement roughness: An analysis of the impact on vehicle dynamic response and driving comfort. *Applied Sciences*, *11*(16), 7582. https://doi.org/10.3390/app11167582